Acta Geologica Sinica (English Edition), 2020, 94(4): 877–883

# Formation Age of the Sujiagou Komatiites in Western Shandong: Further Constraints from SHRIMP U-Pb Zircon Dating on Granitic Dykes

WAN Yusheng[1, *], DONG Chunyan[1], XIE Hangqian[1] and WANG Shijin[2]

[1] *Beijing SHRIMP Center, Institute of Geology, Chinese Academy of Geological Sciences, Beijing 100037, China*
[2] *Shandong Geological Survey Institute, Jinan 250013, China*

**Abstract:** Komatiites are presented as direct evidence for higher mantle temperatures during the Archean. In the North China Craton, komatiites with spinifex structure have been identified only at one locality, i.e. the Sujiagou area, western Shandong. They were considered as formed during the early Neoarchean mainly based on their association with supracrustal rocks considered to be that age. This study carried out SHRIMP U-Pb zircon dating on metamorphosed trondhjemitic and monzogranitic dykes intruding the Sujiagou komatiites, and they have magmatic zircon ages of 2592 ± 12 Ma and 2586 ± 13 Ma respectively. This provides direct evidence that the komatiites formed during the early Neoarchean.

**Key words:** granitic dyke, SHRIMP U-Pb zircon dating, Sujiagou komatiite, Neoarchean, western Shandong

Citation: Wan et al., 2020. Formation Age of the Sujiagou Komatiites in Western Shandong: Further Constraints from SHRIMP U-Pb Zircon Dating on Granitic Dykes. Acta Geologica Sinica (English Edition), 94(4): 877–883. DOI: 10.1111/1755-6724.14549

## 1 Introduction

Komatiites have been discovered in many cratons all over the world, and are treated as direct evidence for higher mantle temperature and heat flux during the Archean period (Barnes and Arndt, 2019; and references therein). In the North China Craton (NCC), komatiites with well-preserved spinifex structure have been identified only in the Sujiagou area, western Shandong (Zhang et al., 1998, 2001). Some ultramafic rocks in other areas (e.g., Helong; Liu, 2001) of the NCC are komatiitic in composition but do not show well-preserved spinifex structures. The komatiites in western Shandong were considered to be formed during the early Neoarchean, mainly based on association with host supracrustal rock of that age, and a previously published Sm-Nd isochron age of 2712 ± 750 Ma (Cao, 1996; Zhang et al., 1998, 2001; Polat et al., 2006) for the komatiites, which has a very large error with the 2712 ± 750 Ma age constraining that the komatiite age could range from Paleoproterozoic to Paleoarchean. Therefore, more precise age constraints are necessary. This study carried out SHRIMP U-Pb zircon dating for the first time on granitic dykes intruding the Sujiagou komatiites, providing more accurate and precise evidence that the komatiites formed during the early Neoarchean.

## 2 Geological Settings

The western Shandong granite-greenstone belt in eastern NCC extends in a northwest-southeast direction and is truncated by the Tanlu Fault (Tancheng-Lujiang Fault) in the east (Fig. 1 inset). Based on rock types and formation ages, three belts in this terrane have been identified (Fig. 1 inset): A late Neoarchean crustally derived granite belt in the northeast (Belt A), a belt mainly composed of 2600–2750 Ma TTG (tonalite-trondhjemite-granodiorite) and supracrustal rocks (Belt B), and a late Neoarchean belt of juvenile rocks in the southwest (Belt C) (Wan et al., 2010, 2011; Ren et al., 2015). The Sujiagou komatiites occur to the ~0.5 km north of Sujiagou village, Mengyin (Belt A).

The Sujiagou komatiites, associated with amphibolite, occur as a large roof pendant in massive granite which has a magmatic zircon age of 2531 ± 8 Ma (S0508, Fig. 1, Wan et al., 2010). The komatiites have been subdivided into spinifex komatiite, brecciated komatiite, lath-shaped komatiite, schistose komatiite and massive komatiite (Fig. 1, Zhang et al., 1998, 2001) or, spinifex komatiite, brecciated komatiite and serpentinized cumulus komatiite (Polat et al., 2006). Yang et al. (2020) divided the spinifex komatiite into random-spinifex komatiite and platy-spinifex komatiite. Spinifex structure is well preserved locally (Fig. 2a). These rocks plot mainly in the field of Al-depleted komatiites in the [$Al_2O_3$] versus [$TiO_2$] diagram and show somewhat large variations in REE (rare earth element) patterns from depletion to enrichment in light REE (Cheng et al., 2006; Polat et al., 2006).

The granitic dykes occur in the supracrustal rocks with a width totalling ~6 m for the dykes that are found in terms of their discrete distribution. They occur between komatiite and amphibolite and underwent strong deformation and weathering, with three types of rocks being identified (Fig. 1). The rocks strike in a northwest-

* Corresponding author. E-mail: wanyusheng@bjshrimp.cn

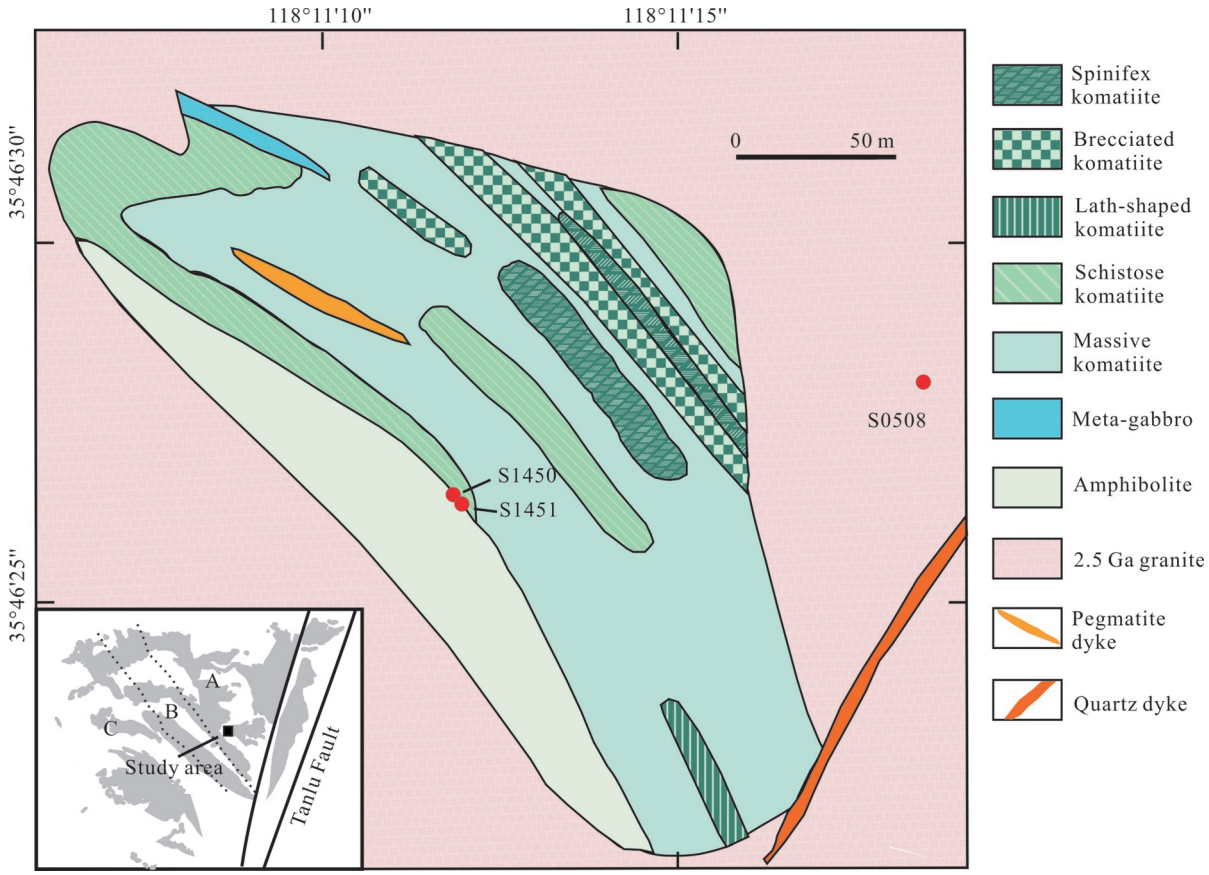


Fig. 1. Geological map of the Sujiagou area, western Shandong (modified after Zhang et al., 2001).

southeast direction, and the amphibolite dips to the southwest with a dip angle of ~70°. Two granitic gneiss samples (S1450, S1451; N35°46′26″/E118°11′11″) were taken from the dykes. Although the samples are taken from the freshest outcrop, they are still strongly weathered (Fig. 2b–e). It is also evident that some thin granitic dykes cut the komatiite (Fig. 2f). The samples used in this study contain only a few ferromagnesian minerals and show intense orientation of minerals and fine-grained mineral aggregates due to strong deformation and recrystallization. Sample S1450 is mainly composed of plagioclase and quartz (trondhjemitic) and sample S1451 contains more K-feldspar (granitic).

## 3 Analytical Methods

Major and trace elements were analyzed at the National Research Center for Geoanalysis, Chinese Academy of Geological Sciences (CAGS), Beijing. X-ray fluorescence (XRF) was used to determine the major elements, and the estimated uncertainties are better than 2%. Trace elements were analyzed by a POEMS ICP-MS. The analytical precision and accuracy were generally better than 5% and 4% for most trace elements, respectively (Qi et al., 2000).

Zircon dating was carried out, guided by cathodoluminescence (CL) imagery, using the SHRIMP II in the Beijing SHRIMP Center, Institute of Geology, CAGS. The analytical procedures and conditions were similar to those described by Williams (1998). A primary $O^{2-}$ ion beam was ~3 nA and the spot size was ~30 μm. Standard zircons M257 (U = 840 ppm; Nasdala et al., 2008) and TEMORA 1 (age = 417 Ma; Black et al., 2003) were used for calibration of elemental abundance and $^{206}Pb/^{238}U$ ratio, respectively. Data for each spot analysis were generated by five scans. A common lead correction was done based on the measured $^{204}Pb$ abundances. Data reduction and assessment were performed using the SQUID and ISOPLOT programs (Ludwing, 2001). The $^{207}Pb/^{206}Pb$ ages were used to assess the age of all samples. Uncertainties for individual analyses are quoted at 1σ, whereas those for weighted mean ages are quoted at the 95% confidence level.

## 4 SHRIMP U-Pb Zircon Dating

### 4.1 Trondhjemitic gneiss (S1450)

The zircons are columnar or prismatic in shape and show oscillatory zoning with rims commonly being darker in cathodoluminescence (CL) images and having stronger recrystallization than the cores (Fig. 3a). Sixteen analyses were performed on 16 zircon grains (Table 1). Eleven analyses on magmatic zircons have U contents of 105–633 ppm and Th/U ratios of 0.17–1.11. The recrystallized rim domains have U contents of 220–744 ppm and Th/U ratios of 0.05–0.12 (1.1, 6.1, 9.1, 11.1, 16.1). This feature of higher U contents and lower Th/U ratios may partly be due to the rims being formed during the fluid stage after magmatism, because some rim domains still show


Fig. 2. Field photographs of Neoarchean rocks in the Sujiagou area, western Shandong.
(a) Komatiite with spinifex structures (Wan et al., 2015); (b) and (c) trondhjemitic gneiss (S1450); (d) and (e) monzogranite gneiss (S1451); (f) ganitic dykes intruding komatiite

oscillatory zoning. Many of them show radiogenic lead loss (Fig. 4a). The analyses near concordia show somewhat large variations in $^{207}Pb/^{206}Pb$ ages, which may be the result of influence of superimposed tectonothermal event(s) on high U+Th zircons. Two analyses close to concordia with the oldest $^{207}Pb/^{206}Pb$ ages (3.1, 7.1) yield a weighted mean $^{207}Pb/^{206}Pb$ age of 2592 ± 12 Ma (MSWD = 0.11), which represents the formation age of the trondhjemite dyke.

### 4.2 Monzogranitic gneiss (S1451)

Zircon grains of this sample are columnar or prismatic in shape and show oscillatory and banded zoning in CL images (Fig. 3b). They show weaker recrystallization compared with those from sample S1450. Fifteen analyses were performed on 15 magmatic zircons (Table 1). They have U contents of 173–772 ppm, Th/U ratios of 0.21–0.65 (analysis 1.1 has a Th/U ratio of 0.06) and high common lead contents of 0.60–10.80%. They show strong radiogenic lead loss but define a discordia line (Fig. 4b). Analyses 4.1 and 10.1, which have the lowest common lead contents, are on concordia and yield a weighted mean $^{207}Pb/^{206}Pb$ age of 2577 ± 19 Ma (MSWD = 0.93). However, the age of 2586 ± 13 Ma for analysis 4.1 may be closer to the "true" formation time of the monzogranite. The high common lead contents and strong radiogenic lead loss may be due to strong weathering of the rock.

## 5 Geochemistry

Sample S1450 is characterized by high contents of $SiO_2$ (72.68 wt%), $Na_2O$ (5.04 wt%) and CaO (3.83 wt%) and low contents of $FeO^t$ (total FeO, 0.53 wt%), MgO (0.09 wt%) and $K_2O$ (0.14 wt%), plotting at the boundary between the tonalite and trondhjemite fields in a modal An-Ab-Or (anorthite-albite-orthoclase) diagram (Fig. 5). It is named as trondhjemitic gneiss because of its minor content of ferromagnesian minerals. It has a low TREE content (total REE) of 43.8 ppm, a relatively high $(La/Yb)_N$ ratio of 28.3 and a strong positive Eu anomaly of 2.16

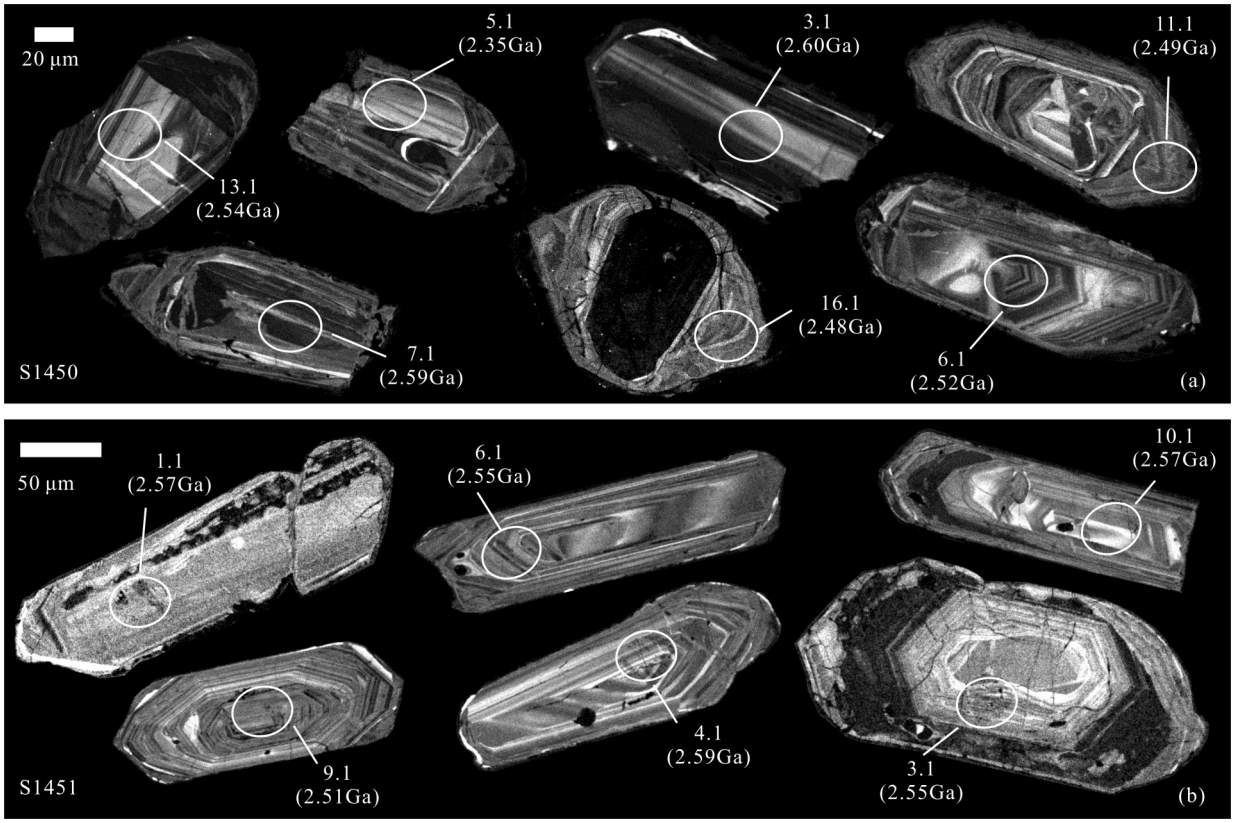


Fig. 3. Cathodoluminescence (CL) images of zircons from granitic dykes in the Sujiagou area, western Shandong.
(a) Trondhjemitic gneiss (S1450); (b) monzogranitic gneiss (S1451)

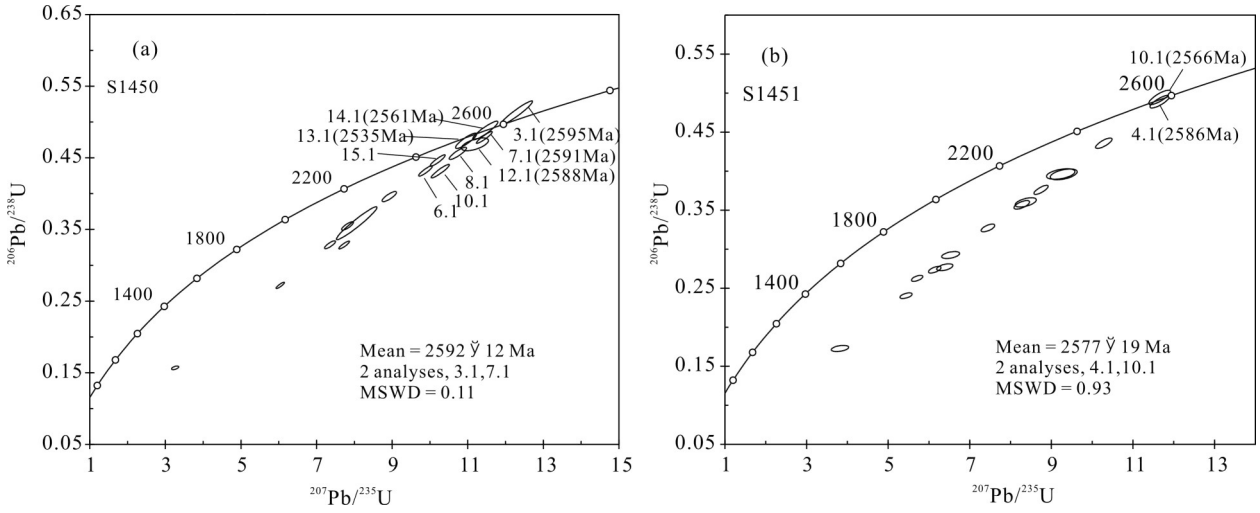


Fig. 4. Concordia diagrams showing SHRIMP U-Pb zircon analyses for granitic dykes in the Sujiagou area, western Shandong.
(a) Trondhjemitic gneiss (S1450); (b) monzogranitic gneiss (S1451)

(Fig. 6a). It shows enrichments in Sr, Th, Nb and Zr in trace element distribution diagram (Fig. 6b).

Sample S1451 has a similar major element composition but is higher in $K_2O$ (2.91 wt%) and lower in CaO (1.16 wt%) and falls in the monzogranite field in the An-Ab-Or diagram (Fig. 5). It has a low TREE content of 42.5 ppm, a low $(La/Yb)_N$ ratio of 16.1 and a negative Eu anomaly of 0.65 (Fig. 6a). It shows enrichment of large ion lithophile elements (K, Rb, Ba and Th) and depletions of Nb, P and Ti (Fig. 6b).

## 6 Discussion and Conclusions

The early Precambrian supracrustal rocks in western Shandong were considered to be composed of the early Neoarchean Taishan "Group", the early Neoarchean Mengjiatun "Formation" and the early Paleoproterozoic Jining "Group". The Taishan "Group" is the most widespread supracrustal sequence in the area and has been subdivided into the Yanlingguan, Shancaoyu and Liuhang "Formations" (Cheng et al., 1982; Hao, 1993; Cao, 1996;

**Table 1 SHRIMP U-Pb data of zircons from granitic dykes in the Sujiagou area, western Shandong**

| Spot | $^{206}Pb_c$ (%) | U (ppm) | Th (ppm) | Th/U | $^{206}Pb^*$ (ppm) | $^{207}Pb^*/^{206}Pb^*$ | ± % | $^{207}Pb^*/^{235}U$ | ± % | $^{206}Pb^*/^{238}U$ | ± % | err corr | $^{206}Pb/^{238}U$ Age (Ma) | $^{207}Pb/^{206}Pb$ Age (Ma) | Discordance (%) |
|---|---|---|---|---|---|---|---|---|---|---|---|---|---|---|---|
| Trondhjemitic gneiss (S1450) | | | | | | | | | | | | | | | |
| S1450-1.1 | 0.74 | 744 | 67 | 0.09 | 229 | 0.1597 | 0.75 | 7.81 | 1.3 | 0.3545 | 1.1 | 0.83 | 1956±19 | 2453±13 | 20 |
| S1450-2.1 | 0.12 | 382 | 206 | 0.56 | 108 | 0.1708 | 0.54 | 7.73 | 1.2 | 0.3282 | 1.1 | 0.90 | 1830±18 | 2565± 9 | 29 |
| S1450-3.1 | 0.00 | 139 | 109 | 0.81 | 61 | 0.1739 | 0.69 | 12.29 | 2.3 | 0.5120 | 2.2 | 0.95 | 2667±48 | 2595±12 | -3 |
| S1450-4.1 | 0.18 | 518 | 181 | 0.36 | 121 | 0.1611 | 0.54 | 6.04 | 1.2 | 0.2718 | 1.1 | 0.89 | 1550±15 | 2467± 9 | 37 |
| S1450-5.1 | 3.43 | 633 | 182 | 0.30 | 88 | 0.1506 | 1.60 | 3.25 | 2.0 | 0.1565 | 1.1 | 0.56 | 937±10 | 2354±28 | 60 |
| S1450-6.1 | 0.18 | 365 | 32 | 0.09 | 136 | 0.1660 | 0.52 | 9.88 | 1.2 | 0.4315 | 1.1 | 0.90 | 2312±21 | 2518± 9 | 8 |
| S1450-7.1 | 0.02 | 332 | 89 | 0.28 | 137 | 0.1734 | 0.44 | 11.44 | 1.2 | 0.4785 | 1.2 | 0.93 | 2521±24 | 2591± 7 | 3 |
| S1450-8.1 | 0.14 | 168 | 54 | 0.33 | 66 | 0.1707 | 0.68 | 10.74 | 1.4 | 0.4561 | 1.2 | 0.88 | 2422±25 | 2565±11 | 6 |
| S1450-9.1 | 0.35 | 220 | 25 | 0.12 | 68 | 0.1630 | 1.20 | 8.06 | 4.4 | 0.3590 | 4.2 | 0.96 | 1975±72 | 2487±20 | 21 |
| S1450-10.1 | 0.22 | 310 | 228 | 0.76 | 115 | 0.1727 | 0.57 | 10.27 | 1.6 | 0.4312 | 1.4 | 0.93 | 2311±28 | 2584±10 | 11 |
| S1450-11.1 | 0.77 | 314 | 27 | 0.09 | 108 | 0.1635 | 0.80 | 8.91 | 1.4 | 0.3953 | 1.2 | 0.83 | 2147±22 | 2492±13 | 14 |
| S1450-12.1 | 0.97 | 220 | 35 | 0.17 | 90 | 0.1731 | 1.70 | 11.16 | 2.1 | 0.4676 | 1.3 | 0.60 | 2473±26 | 2588±29 | 4 |
| S1450-13.1 | -0.01 | 105 | 25 | 0.25 | 43 | 0.1677 | 0.80 | 10.96 | 1.7 | 0.4738 | 1.5 | 0.88 | 2500±31 | 2535±13 | 1 |
| S1450-14.1 | 0.16 | 112 | 121 | 1.11 | 47 | 0.1703 | 0.80 | 11.46 | 1.9 | 0.4879 | 1.8 | 0.91 | 2562±37 | 2561±13 | 0 |
| S1450-15.1 | 0.11 | 275 | 121 | 0.45 | 106 | 0.1658 | 0.52 | 10.20 | 1.3 | 0.4462 | 1.2 | 0.91 | 2378±24 | 2516± 9 | 5 |
| S1450-16.1 | 0.23 | 363 | 18 | 0.05 | 103 | 0.1623 | 0.74 | 7.35 | 1.3 | 0.3285 | 1.1 | 0.83 | 1831±18 | 2480±12 | 26 |
| Monzogranitic gneiss (S1451) | | | | | | | | | | | | | | | |
| Spot | $^{206}Pb_c$ (%) | U (ppm) | Th (ppm) | Th/U | $^{206}Pb^*$ (ppm) | $^{207}Pb^*/^{206}Pb^*$ | ± % | $^{207}Pb^*/^{235}U$ | ± % | $^{206}Pb^*/^{238}U$ | ± % | err corr | $^{206}Pb/^{238}U$ Age (Ma) | $^{207}Pb/^{206}Pb$ Age (Ma) | Discordance (%) |
| S1451-1.1 | 0.63 | 271 | 15 | 0.06 | 102 | 0.1712 | 0.82 | 10.27 | 1.3 | 0.4351 | 1.0 | 0.78 | 2329±20 | 2570±14 | 9 |
| S1451-2.1 | 10.80 | 772 | 478 | 0.64 | 128 | 0.1604 | 3.40 | 3.81 | 3.6 | 0.1715 | 1.5 | 0.42 | 1021±14 | 2465±55 | 59 |
| S1451-3.1 | 0.91 | 326 | 115 | 0.36 | 106 | 0.1687 | 0.83 | 8.74 | 1.3 | 0.3754 | 1.0 | 0.78 | 2055±18 | 2545±14 | 19 |
| S1451-4.1 | 0.60 | 173 | 95 | 0.57 | 73 | 0.1729 | 0.80 | 11.64 | 1.4 | 0.4882 | 1.1 | 0.81 | 2563±23 | 2586±13 | 1 |
| S1451-5.1 | 4.90 | 248 | 68 | 0.28 | 89 | 0.1689 | 2.20 | 9.14 | 2.4 | 0.3920 | 1.1 | 0.47 | 2132±20 | 2549±36 | 16 |
| S1451-6.1 | 2.37 | 261 | 82 | 0.32 | 83 | 0.1687 | 1.70 | 8.34 | 2.0 | 0.3584 | 1.1 | 0.55 | 1974±19 | 2546±28 | 22 |
| S1451-7.1 | 0.62 | 334 | 113 | 0.35 | 103 | 0.1682 | 1.10 | 8.27 | 1.5 | 0.3564 | 1.0 | 0.67 | 1965±17 | 2540±19 | 23 |
| S1451-8.1 | 3.61 | 506 | 194 | 0.40 | 108 | 0.1641 | 1.50 | 5.43 | 1.8 | 0.2395 | 1.0 | 0.56 | 1384±12 | 2500±25 | 45 |
| S1451-9.1 | 2.17 | 437 | 146 | 0.35 | 126 | 0.1650 | 1.10 | 7.42 | 1.5 | 0.3260 | 1.0 | 0.67 | 1819±16 | 2509±18 | 28 |
| S1451-10.1 | 0.60 | 180 | 113 | 0.65 | 77 | 0.1709 | 0.89 | 11.63 | 1.5 | 0.4936 | 1.2 | 0.82 | 2586±27 | 2566±15 | -1 |
| S1451-11.1 | 2.53 | 426 | 158 | 0.38 | 103 | 0.1627 | 1.30 | 6.13 | 1.6 | 0.2729 | 1.0 | 0.63 | 1555±14 | 2486±21 | 37 |
| S1451-12.1 | 1.94 | 475 | 184 | 0.40 | 109 | 0.1576 | 1.30 | 5.70 | 1.6 | 0.2620 | 1.0 | 0.61 | 1500±13 | 2432±22 | 38 |
| S1451-13.1 | 3.97 | 440 | 111 | 0.26 | 115 | 0.1620 | 2.00 | 6.51 | 2.2 | 0.2908 | 1.0 | 0.47 | 1646±15 | 2479±32 | 34 |
| S1451-14.1 | 4.66 | 528 | 106 | 0.21 | 132 | 0.1674 | 1.80 | 6.36 | 2.0 | 0.2752 | 1.1 | 0.53 | 1567±15 | 2535±29 | 38 |
| S1451-15.1 | 3.14 | 205 | 96 | 0.48 | 72 | 0.1704 | 2.10 | 9.25 | 2.3 | 0.3931 | 1.2 | 0.51 | 2137±21 | 2563±34 | 17 |

Note: 1) Common lead corrected using measured $^{204}Pb$; 2) $^{206}Pb^*$ is radiogenic lead; 3) discordance (%) is defined as [(1– ($^{206}Pb/^{238}U$)age)/($^{207}Pb/^{206}Pb$)age]×100

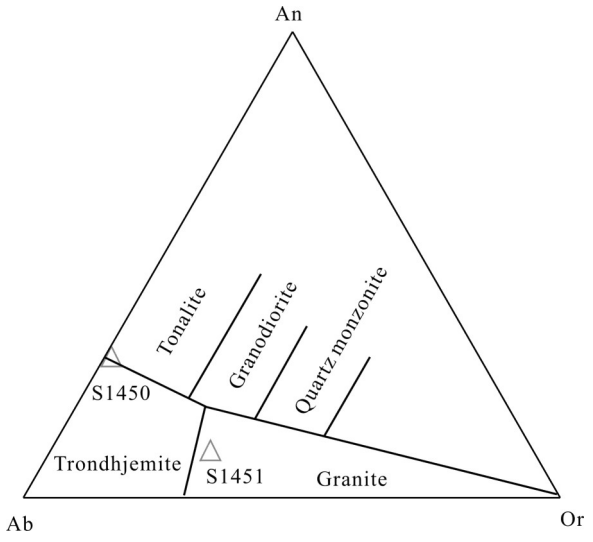


Fig. 5. An-Ab-Or diagram of granitic dykes in the Sujiagou area, western Shandong (after Barker, 1979).

Zhang et al., 1998, 2001; Du et al., 2003, 2005; Polat et al., 2006). According to available zircon dating results, the timing of deposition and eruption of the supracrustal rocks were redefined by Wan et al. (2012). The Neoarchean supracrustal rocks in western Shandong show different rock associations: 1) the supracrustal rocks formed during the early Neoarchean (2.70–2.75 Ga) are mainly composed of amphibolite and meta-ultramafic rocks; and 2) the late Neoarchean (2.52–2.55 Ga) supracrustal rocks mainly consist of fine-grained biotite gneiss, conglomerate, BIF and felsic meta-volcanic rocks (Wan et al., 2012). Based on the study in the Yanlingguan area, Xintai, Cheng et al. (1982) indicated for the first time that the meta-ultramafic rocks in the supracrustal rocks contain metamorphosed komatiitic rocks. They further shown that blastospinifex structures may be preserved in some komatiitic rocks (Cheng and Xu, 1991). In this study we provide magmatic zircon ages of ~2.6 Ga for the granitic dykes that intruded the komatiites, demonstrating that the komatiites were formed during 2.70–2.75 Ga, because no supracrustal rocks of 2.60–2.70 Ga have been found in western Shandong and even the entire North China Craton.

The two samples were taken from the same outcrop but show differences in whole-rock element compositions and zircon petrography. The differences cannot be explained in terms of late strong deformation, therefore, they represent different granitic dykes. We suggest that different types of

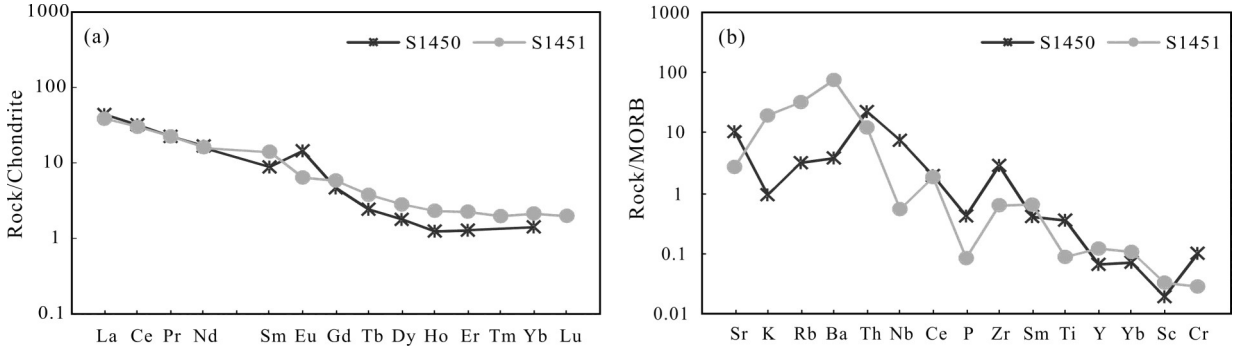


Fig. 6 Geochemical diagrams of granitic dykes in the Sujiagou area, western Shandong.
(a) REE pattern; (b) trace element distribution pattern. REE-normalizing values after Sun and McDonough (1989) and MORB-normalizing values after Pearce (1983).

**Table 2 Element compositions of granitic dykes in the Sujiagou area, western Shandong**

| Sample no. | S1450 | S1451 |
|---|---|---|
| Rock type | Trondhjemitic gneiss | Monzogranitic gneiss |
| $SiO_2$ | 72.68 | 74.2 |
| $TiO_2$ | 0.53 | 0.13 |
| $Al_2O_3$ | 15.76 | 14.18 |
| $Fe_2O_3$ | 0.27 | 0.93 |
| FeO | 0.29 | 0.22 |
| MnO | 0.01 | 0.01 |
| MgO | 0.09 | 0.28 |
| CaO | 3.83 | 1.16 |
| $Na_2O$ | 5.04 | 4.09 |
| $K_2O$ | 0.14 | 2.91 |
| $P_2O_5$ | 0.05 | 0.01 |
| $CO_2$ | 0.99 | 0.76 |
| $H_2O^+$ | 0.37 | 1.04 |
| Total | 100.05 | 99.92 |
| Cr | 25 | 7 |
| Ni | 8 | 5 |
| Sc | 1 | 1 |
| Rb | 6 | 64 |
| Ba | 76 | 1499 |
| Sr | 1254 | 325 |
| Nb | 26.3 | 1.89 |
| Ta | 1.34 | 0.18 |
| Hf | 6.02 | 2.73 |
| Zr | 258 | 56.3 |
| Y | 1.97 | 3.6 |
| Th | 4.49 | 2.44 |
| U | 0.88 | 2.93 |
| La | 10.30 | 9.05 |
| Ce | 19.40 | 18.30 |
| Pr | 2.12 | 2.12 |
| Nd | 7.75 | 7.48 |
| Sm | 1.34 | 2.13 |
| Eu | 0.83 | 0.37 |
| Gd | 0.95 | 1.19 |
| Tb | 0.09 | 0.14 |
| Dy | 0.45 | 0.71 |
| Ho | 0.07 | 0.13 |
| Er | 0.21 | 0.37 |
| Tm | <0.05 | 0.05 |
| Yb | 0.24 | 0.36 |
| Lu | <0.05 | 0.05 |
| TREE | 43.8 | 42.5 |
| (La/Yb)n | 28.3 | 16.6 |
| Eu/Eu* | 2.16 | 0.65 |

Notes: Major element in %, trace and REE elements in ppm

~2.6 Ga granitic dykes intruded the komatiites together and then underwent strong later deformation, resulting in parallelization of all rocks. It is speculated that the timing of the deformation occurred at the end of the Neoarchean for the reasons: 1) sample S1450 has the recrystallized zircon domains with the youngest age of 2535 Ma (13.1, discordance = 1%); and 2) the Sujiagou komatiites occur in Belt A, which underwent strong tectonothermal event of the late Neoarchean (Dong et al., 2017).

## Acknowledgements

This paper is to honour Academician Li Tingdong, on the occasion of his 90th birthday (2020), who has made great contributions to geology in China. We thank Yang Chun, Zhang Zhichao and Zhou Liqing for mount making and zircon CL imaging. We also appreciate the technical support of Liu Jianhui and Che Xiaochao for the smooth operation of the SHRIMP instrument during zircon dating. Thanks are also to Yang Chonghui and Wang Xiaolei for helpful comments. This study was financially supported by the Key Program of the Ministry of Land and Resources of China (DD20190370, DD20190009, DD20190358, DD20190003).

Manuscript received Apr. 5, 2020
accepted Jun. 5, 2020
associate EIC: DING Xiaozhong
edited by ZHANG Yuxu

## References

Barker, F., 1979. Trondhjemite: definition, environment and hypotheses of origin. In: Barker, F. (ed.), Trondhjemites, Dacites, and Related Rocks. Elsevier, 1–12.

Barnes, S.J., and Arndt, N.T., 2019. Distribution and geochemistry of komatiites and basalts through the Archean. In: Van Kranendonk, M.J., Smithies, R.H., and Bennett, V. (eds.), Earth's Oldest Rocks (second edition). Elsevier, 103–133.

Black, L.P., Kamo, S.L., Allen, C.M., Aleinikoff, C.M., Davis, D.W., Korsch, R.J., and Foudoulis, C., 2003. TEMORA 1: a new zircon standard for Phanerozoic U-Pb geochronology. Chemical Geology, 200: 155–170.

Cao, G.Q., 1996. Early Precambrian geology of western Shandong. Beijing: Geological Publishing House, 1–210 (in Chinese).

Cheng, Y.Q., Sheng, Q.H., and Wang, Z.J., 1982. Preliminary study of the metamorphosed basic volcano-sedimentary Yanlingguan Formation of the Taishan Group of Xintai, Shandong. Beijing: Geological Publishing House, 1–72 (in Chinese).

Cheng, Y.Q., and Xu, H.F., 1991. Some new knowledge of

komatiitic rocks in the Late Archean Yanlinguan Formation in Xintai, Shandong. Chinese Geology, 18: 31–32.
Cheng, S.H., Li, J.H., Chen, Z., and Niu, X.L., 2006. Geochemical characteristics of the komatiites in Mengyin, Shandong Province, and their implications. Acta Petrologica et Mineralogica, 25: 119–126.
Dong, C.Y., Xie, H.Q., Kröner, A., Wang, S.J., Liu, S.J., Xie, S.W., Song, Z.Y., Ma, M.Z., Liu, D.Y., and Wan, Y.S., 2017. The complexities of zircon crystllazition and overprinting during metamorphism and anatexis: an example from the late Archean TTG terrane of western Shandong Province, China. Precambrian Research, 300: 181–200.
Hao, Z.G., 1993. A brief introduction to the Symposium on Archean komatiite and related meta-basalts in western Shandong. Geological Review, 39(2): 186.
Liu, J.H., 2001. Discovery and identification of Helong ultramafic komatiite in the eastern part of North China Block. Geological Review, 47(4): 420–424.
Ludwig, K.R., 2001. Isoplot/Ex(rev). 2.49: a geochronological toolkit for Microsoft Excel. Berkeley Geochronological Center: Special Publication 1a, 1–58.
Nasdala, L., Hofmeister, W., Norberg, N., Mattinson, J.M., Corfu, F., Dor, W., Kamo, S.L., Kennedy, A.K., Kronz, A., Reiners, P.W., Frei, D., Kosler, J., Wan, Y.S., Goze, J., Hoer, T., Kröner, A., and Valley, J.W., 2008. Zircon M257-a homogeneous natural reference material for the ion microprobe U-Pb analysis of zircon. Geostandards and Geoanalytical Research, 32: 247–265.
Pearce, J.A., 1983. The role of sub-continental lithosphere in magma genesis at active continental margins. In: Hawkesworth, C.J., and Norry, M.J. (eds.), Continental Basalts and Mantle Xenoliths. Cambridge: Shiva Publish Limited, 230–249.
Polat, A., Li, J., Fryer, B., Kusky, T., Gagnon, J., and Zhang, S., 2006. Geochemical characteristics of the Neoarchean (2800–2700 Ma) Taishan greenstone belt, North China Craton: Evidence for plume-craton interaction. Chemical Geololy, 230: 60–87.
Qi, L., Hu, J., and Gregoire, D.C., 2000. Determination of trace elements in granites by inductively coupled plasma mass spectrometry. Talanta, 51: 507–513.
Ren, P., Xie, H.Q., Wang, S.J., Dong, C.Y., Ma, M.Z., Liu, D.Y., and Wan, Y.S., 2015. 2.5~2.7 Ga tectonothermal events in western Shandong: Geology and zircon SHRIMP dating of TTG rocks in Huangqian reservoir, Taishan Mountain. Geological Review, 61(5):1068–1078.
Sun, S.S., and McDonough, W.F., 1989. Chemical and isotopic systematics of oceanic basalts: implications for mantle composition and processes. In: Saunders, A.D., and Norry, M.J. (eds.), Magmatism in the Ocean Basins.London: Geological Society of London, Special Publication, 313–345.
Wan, Y.S., Liu, D.Y., Wang, S.J., Dong, C.Y., Yang, E.X., Wang, W., Zhou, H.Y., Ning, Z.G., Du, L.L., Yin, X.Y., Xie, H.Q., and Ma, M.Z., 2010. Juvenile magmatism and crustal recycling at the end of the Neoarchean in western Shandong Province, North China Craton: evidence from SHRIMP zircon dating. American Journal of Science, 310: 1503–1552.
Wan, Y.S., Liu, D.Y., Wang, S.J., Yang, E.X., Wang, W., Dong, C.Y., Zhou, H.Y., Du, L.L., Yang, Y.H., and Diwu, C.R., 2011. ~2.7 Ga juvenile crust formation in the North China Craton (Taishan-Xintai area, western Shandong Province): Further evidence of an understated event from zircon U-Pb dating and Hf isotope composition. Precambrian Research, 186: 169–180.
Wan, Y.S., Wang, S.J., Liu, D.Y., Wang, W., Kröner, A., Dong, C.Y., Yang, E.X., Zhou, H.Y., Xie, H.Q., and Ma, M.Z., 2012. Redefinition of depositional ages of Neoarchean supracrustal rocks in western Shandong Province, China: SHRIMP U-Pb zircon dating. Gondwana Research, 21: 768–784
Wan, Y.S., Liu, D.Y., Dong, C.Y., Xie, H.Q., Kröner, A., Ma, M.Z., Liu, S.J., Xie, S.W., and Ren, P., 2015. Formation and evolution of Archean continental crust of the North China Craton. In: Zhai, M.G. (ed.), Precambrian geology of China. Springer, 59–136.
Williams, I.S., 1998. U-Th-Pb geochronology by ion microprobe. In: McKibben, M.A., Shanks, W.C., and Ridley, W.I. (eds.), Applications of microanalytical techniques to understanding mineralizing processes. Review Economic Geology, 7: 1–35.
Yang, L.H., Tian, W., Gou, G.T., Liu, S.W., Li, J., Chen, M.M., and Wang, B., 2020. Volcanic succession and petrology of the Yanlingguan komatiite from the North China Craton. Geological Journal (in press).
Zhang, R.S., Si, R.J., Song, B.Z., and Liu, S.M., 1998. Komatiite in Sujiagou village of Mengyin County. Shandong Geology, 14: 26–33 (in Chinese with English abstract).
Zhang, R.S., Tang, H.S., Kong, L.G., Gan, Y.J., and Song, B.Z., 2001. Characteristics and significance of the Sujiagou komatiite at Menying, Shandong. Regional Geology of China, 20: 26–33 (in Chinese with English abstract).

## About the first and corresponding author

WAN Yusheng is a senior researcher in the Beijing SHRIMP Centre, Institute of Geology, Chinese Academy of Geological Sciences, Beijing. His research interest is mainly in the geology, geochronology and geochemistry of the basement of the North China Craton to understand its early Precambrian geological evolution.